Supplementary Material: *A quorum sensing active matter in a confined geometry*

Yuxin Zhou[1], Yunyun Li [1*] and Fabio Marchesoni[1,2†]

[1] *MOE Key Laboratory of Advanced Micro-Structured Materials and Shanghai Key Laboratory of Special Artificial Microstructure Materials and Technology, School of Physics Science and Engineering, Tongji University, Shanghai 200092, China and*

[2] *Dipartimento di Fisica, Università di Camerino, I-62032 Camerino, Italy*

(Dated: October 4, 2023)

Abstract

This file contains supplementary information to assist reviewers and editors to process the manuscript entitled "Quorum sensing and pattern formation of active matter in a confined geometry", submitted for publication in the Chinese Physical Letters. Part of the contents hereby will be submitted for publication as a regular follow-up paper.

PACS numbers:

*Electronic address: yunyunli@tongji.edu.cn

†Electronic address: fabio.marchesoni@pg.infn.it

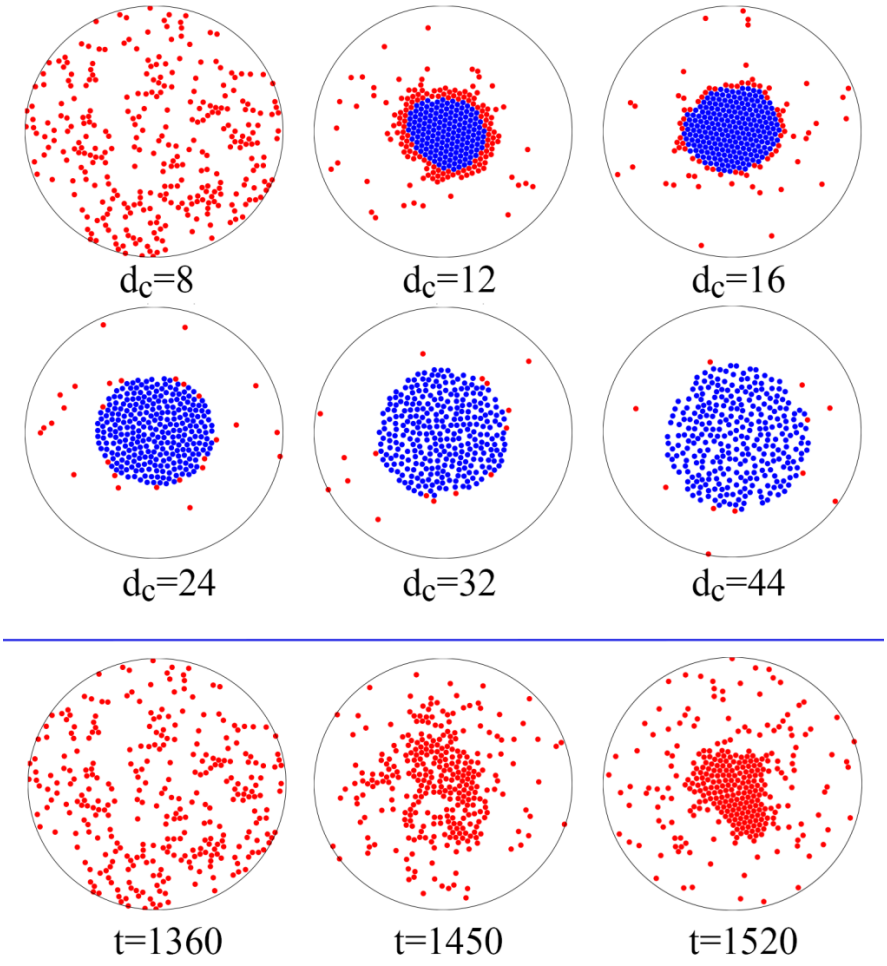

FIG. 1: Top panels: snapshots of a suspension undergoing quorum-sensing induced active-passive transition for different values of the horizon distance, d_c, and $p(\phi) = \delta(\phi)$, i.e., $\lambda = \infty$. All snapshots were taken at time $t = 2 \times 10^4$. Bottom panels: three consecutive snapshots of the above suspension for $d_c = 8$. In all panels, active/passive particles are denoted by red/blue circles and the remaining simulation parameters are: $\alpha = \pi$, $D_\theta = 0.001$, $v_0 = 0.5$, $R = 45$, $r_0 = 1$, $N = 304$, and $D_0 = 0.01$.

We present supplementary numerical results, which further support the conclusions of the main text, but were not shown there due to space limitations.

I. QUORUM SENSING PROTOCOL

The quorum sensing threshold, $P_0(\alpha)$, has been fixed with reference to a confined suspension. Indeed, for a uniform distribution, $P_i(\alpha)$ in Eq. (3) of the main text is maximum when $d_c = R$ and i is placed at the center of the cavity. Then, assuming the continuum limit, the sum there can be approximated to

$$\sum_{j \in V_i^\alpha} \frac{1}{2\pi r_{ij}} \to \int_0^R \frac{\rho_0}{2\pi r_{ij}} dA_{ij}, \tag{1}$$

with $dA_{ij} = 2\alpha_{ij} dr_{ij}$, hence Eq. (4) of the main text. For practical purposes, $P_0(\alpha)$ can be multiplied by an arbitrary scaling factor, as more appropriate.

II. THE ROLE OF d_c

The role of the horizon distance d_c is illustrated in Fig. 2 of the main text. A (red) curve separates region I, where passive clusters never form, from regions II-IV, where passive clusters of different density have been observed. In the top panels of Fig. 1 we display snapshots of the suspension for $\lambda = \infty$, taken at $t = 2 \times 10^4$. In the notation of Eq. (2), main text, $\lambda = \infty$ means that the scattering angle distribution is approximated by $p(\phi) = \delta(\phi)$, that is the scattered particles are redirected toward the center of the cavity. The emergence of a dense passive cluster core is apparent as d_c is increased from region I into region III (steady hexatic phase). At larger d_c, such close packed clusters are replaced by disordered, larger clusters (liquid phase). The fraction of the surviving active particles diminishes with increasing d_c; the active-passive transitions take place mostly along the dynamically fluctuating border of the clusters, as confirmed by the relevant radial distributions of the active particles (an example is shown in Fig. 1(d) of the main text). As anticipated in the main text, in region I (small d_c) for large λ (strong boundary lensing regime) we observed transient clustering, but no active-passive transitions (Fig. 1, bottom panels). Such clusters are rapidly forming and dissolving and are all made of active particles.

III. THE ROLE OF D_θ

As anticipated in the text, increasing D_θ, that is, shortening the persistence time of the self-propulsion mechanism, is expected to hamper the active-to-passive transition, thus

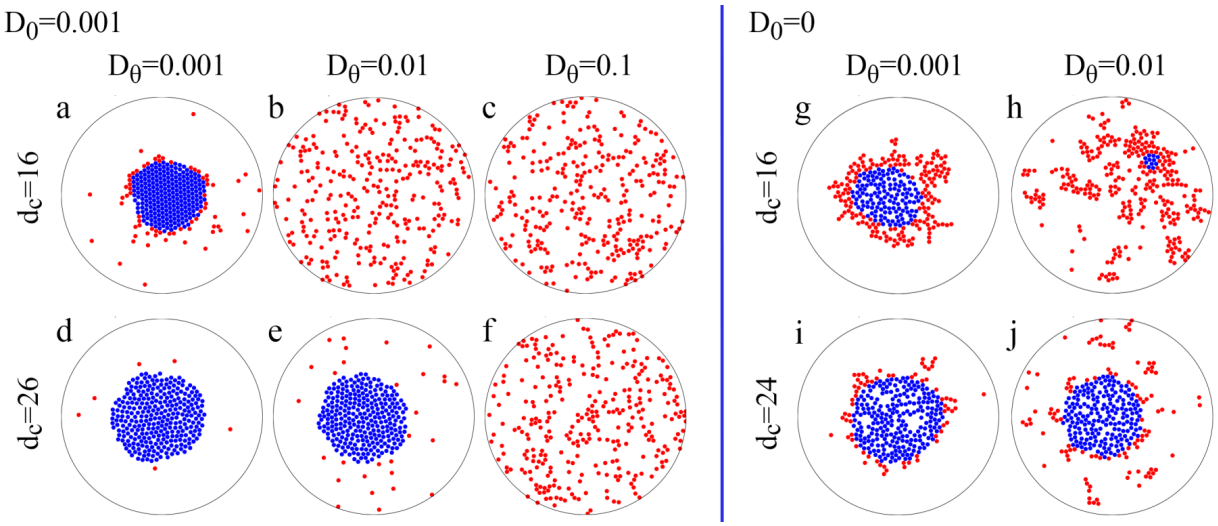

FIG. 2: Snapshots of an active suspension undergoing quorum sensing for different values of D_θ and d_c, with and without thermal noise ($D_0 = 0.001$ in the l.h.s. panels, taken at time $t = 2 \times 10^4$, and $D_0 = 0$ in the r.h.s. panels, taken at $t = 10^5$). In all panels, active/passive particles are denoted by red/blue circles and the remaining simulation parameters are: $\alpha = \pi$, $v_0 = 0.5$, $R = 45$, $r_0 = 1$, and $N = 304$.

raising the corresponding clustering threshold d_c vs. λ in Fig. 2 of the main text. The simulation results reported in Fig. 2 validate one's expectations both in the presence, $D_0 > 0$, and in the absence of thermal noise, $D_0 = 0$.

The cluster showed in panel (h) undergoes the time oscillations typical of region IV, with the emergence of short-lived small passive cores (drawn in blue). All other patterns reported in figure are stationary, that is, fluctuating in time, but globally stable.

IV. THE ROLE OF α

The role of the visual angle, α, can be regarded as a measure of the non-reciprocal character of the particle interactions induced by sensing. As discussed in the main text, a large value of α emphasizes the difference in the confining action exerted by the active particles entering or leaving the forming cluster. In particular, an active particle re-injected toward the cavity center has little chance to sense any other particle, if its visual angle is narrower than the perceived angular distance between its neighbours (which for a uniform

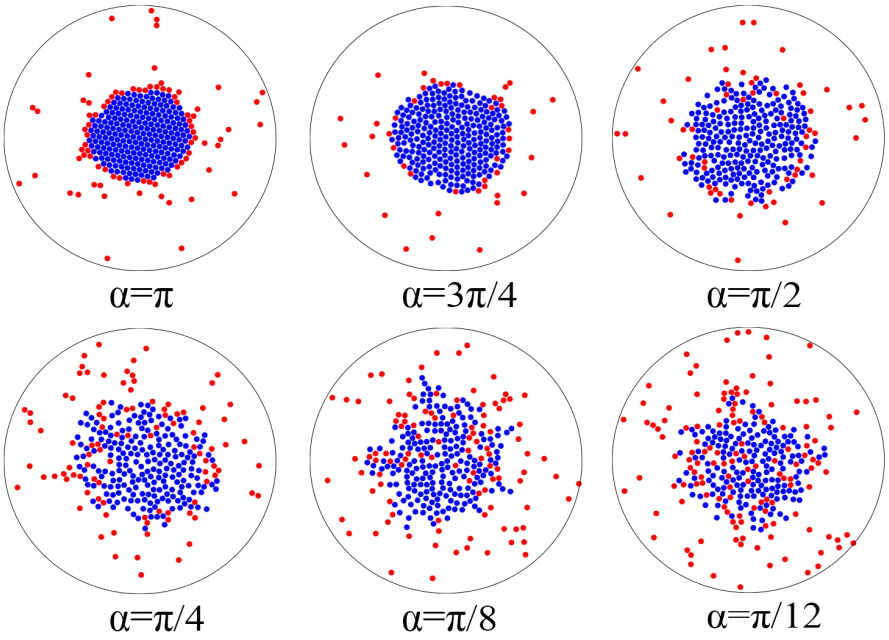

FIG. 3: Snapshots at $t = 2 \times 10^4$ of an active suspension undergoing quorum sensing for different values of the visual angle α and fixed horizon distance, $d_c = 16$. In all panels, active/passive particles are denoted by red/blue circles and the remaining simulation parameters are: $D_\theta = 0.001$, $v_0 = 0.5$, $R = 45$, $r_0 = 1$, $N = 304$ and $D_0 = 0.01$.

distribution is of the order of $d_c\sqrt{\rho_0}$).

Not surprisingly, upon lowering α, the active particles hitting the cluster seem to penetrate deeper inside it, thus causing its progressive fragmentation (see Figs. 3). This mechanism is apparent in Fig. 4 for small visual angles, $\alpha < \pi/2$.

As a consequence, α strongly affects the (average) fraction of the active particles making the active-to-passive transition, as shown in Fig. 5 of the main text. The existence of an optimal visual angle that maximizes the asymptotic value of the ratio $N_p(t)/N$, can be explained by noticing that, for an active particle directed against a forming cluster, the transition threshold, $P_0(\alpha)$, is proportional to α, whereas increasing α from $\pi/2$ to π leaves the actual value of the sensing function largely unaltered [compare Eqs. (3) and (4) in the main text].

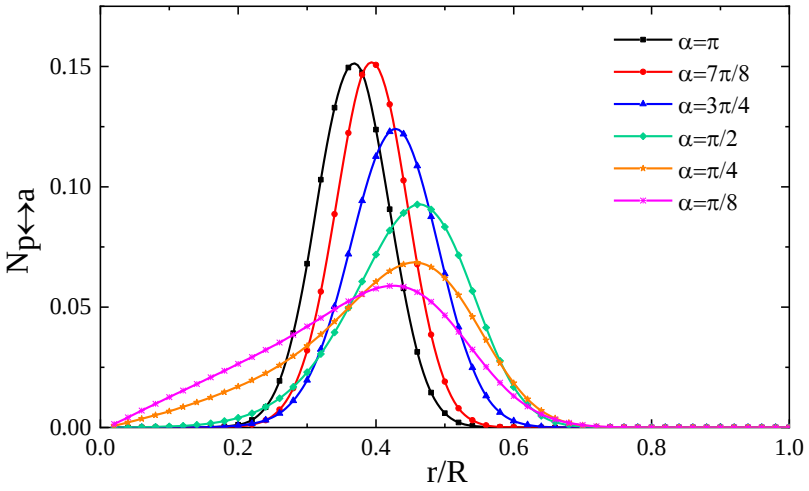

FIG. 4: Number of active-passive transition events per unit of time and area taking place at a distance r from the cavity center for different α. Distributions have been averaged over time in the steady-state regime (see Fig. 3 of the main text). The remaining simulation parameters are: $D_\theta = 0.001$, $\lambda = \infty$, $d_c = 16$, $v_0 = 0.5$, $R = 45$, $r_0 = 1$, $N = 304$ and $D_0 = 0.01$.